Electronic Supplementary Information

Synthetic method, growth mechanism and electrochemical properties of $PbSnS_2$ nanosheets for supercapacitors

Experimental section

Fabrication: $PbSnS_2$ was synthesized according to a facile one-step hydrothermal method, in which 1 mmol stannous chloride ($SnCl_2 \cdot 2H_2O$), 1 mmol lead chloride ($PbCl_2$) and 3 mmol thiourea ($SC(NH_2)_2$) were dissolved in 40 mL ultrapure water to obtain a clear solution. After homogenous magnetic stirring for 30 min, the mixed solution was transferred into a Teflon-lined stainless-steel autoclave, which was hydrothermally treated at 180 °C for 6 hours in the resistance furnace. The obtained products were centrifuged out at 2000 rpm for 3 min every time, then washed by ultrapure water. And this process was repeated for 8 times. Finally, the specimens dried in a vacuum oven at 50 °C for 24 hours. The pure SnS was prepared by a similar method as described above, specifically, there is 2 mmol $SnCl_2 \cdot 2H_2O$ and 4 mmol $SC(NH_2)_2$, and the temperature of reaction raised to 200 °C.

Characterization: The field emission scanning electron microscopy (FE-SEM, Zeiss Merlin Compact) equipped with an energy-dispersive spectrometer (EDS, Oxford Atec X-max 50), transmission electron microscopy (TEM, JEOL JEM-2100), X-ray diffraction (XRD, Rigaku Ultima-IV) using Cu K_α radiation at a scan rate of 10 °/min, X-ray photoelectron spectroscopy (XPS, ThermoFisher ESCA2000) with a CLAM4 hemispherical analyser and Raman analysis (Invia, Renishaw) with 514 nm wavelength laser were utilized to analyze the morphologies, microstructures, composition of the as-obtained electrodes respectively.

Electrochemical tests: The as-prepared $PbSnS_2$ was mixed with 20 wt.% conducting agent (10 wt.% acetylene black and 10 wt.% carbon fiber) and 5 wt.% poly tetra fluoro ethylene (PTFE) latex as binder, for the further electrochemical properties evaluation. A slurry composed of the above mixtures was subsequently spread on a nickel foam with the area of 1 cm^2. And then, the nickel foam was dried in vacuum oven at room temperature for 0.5 h to remove the solvent and finally pressed to ensure good adherence between the electrode material and nickel foam current collector.

The cyclic voltammetry (CV), galvanostatic charge/discharge measurements (GCD) and electrochemical impedance spectroscopy (EIS) were conducted in a 2M KOH solution at room temperature. An electrochemical workstation (Donghua, DH7000) with a three electrode configuration was utilized, where the as-prepared electrode, Ag/AgCl standard electrode and Pt plate acted as the working electrode, reference electrode and the counter electrode respectively. CV tests were performed over a voltage range of 0 to 0.6 V, and the scan rates ranged from 1 to 100 $mV \cdot s^{-1}$. GCD measurements were conducted at various current densities from 1 to 20 $A \cdot g^{-1}$. Capacitance retention was measured on a supercapacitor analyser (Neware, CT-4000).

Figure captions

Tab. S1 A comparison among capacitance of related materials for supercapacitors.

No.	Materials	Scan rate/current density	Capacitance	Retention	Ref.
1	CuS-AC	0.5 $A \cdot g^{-1}$	247.0 $F \cdot g^{-1}$	92 % (5, 000 cycles)	[1]
2	(p)-CoS_2/CNT	5 $mV \cdot s^{-1}$	839 $F \cdot g^{-1}$	82.9 % (5, 000 cycles)	[2]
3	NiS-NF/AC	5 $mV \cdot s^{-1}$	94.2 $F \cdot g^{-1}$	90 % (2, 000 cycles)	[3]
4	WS_2/RGO	2 $mV \cdot s^{-1}$	350.0 $F \cdot g^{-1}$	- (1, 000 cycles)	[4]
5	PbS	50 $mV \cdot s^{-1}$	241.0 $F \cdot g^{-1}$	95.9 % (6, 000 cycles)	[5]
6	M-MoS_2	5 $mV \cdot s^{-1}$	380.0 $F \cdot g^{-1}$	88 % (10, 000 cycles)	[6]
7	mesoporous MoS_2	1 $A \cdot g^{-1}$	376.0 $F \cdot g^{-1}$	80 % (2, 000 cycles)	[7]
8	Mo-SnS_2	1 $A \cdot g^{-1}$	213.4 $F \cdot g^{-1}$	89% (1, 000 cycles)	[8]
9	SnS_2/SnO_2	2 $A \cdot g^{-1}$	149.0 $F \cdot g^{-1}$	92 % (3, 000 cycles)	[9]
10	MoO_2/MoS_2	5 $mV \cdot s^{-1}$	433.3 $F \cdot g^{-1}$	84.41 % (5, 000 cycles)	[10]
11	SnS_2/g-C_3N_4	1 $A \cdot g^{-1}$	210.3 $F \cdot g^{-1}$	84 % (1, 500 cycles)	[11]
12	SnS_2/MoS_2	2.35 $A \cdot g^{-1}$	105.7 $F \cdot g^{-1}$	90.4 % (1, 000 cycles)	[12]
13	SnS nanorods	0.5 $mA \cdot cm^{-2}$	~ 70 $F \cdot g^{-1}$	60 % (500 cycles)	[13]
14	SnS/carbon	200 $mA \cdot g^{-1}$	36.16 $F \cdot g^{-1}$	-	[14]
15	SnS	5 $mV \cdot s^{-1}$	288.1 $F \cdot g^{-1}$	66.10 % (100, 000 cycles)	this work
16	$PbSnS_2$	5 $mV \cdot s^{-1}$	678.6 $F \cdot g^{-1}$	95.50 % (100, 000 cycles)	this work

[1] G. X. Wang, M. Y. Zhang, L. Lu, H. F. Xu, Z. Y. Xiao, S. Liu, S. P. Gao, and Z. H. Yu, *ChemNanoMat*, 2018, **4**, 964.

[2] K. Y. Zou, Y. C. Liu, Y. F. Jiang, C. Y. Yu, M. L.Yue, and Z. X. Li, *Inorg. Chem.*, 2017, **56**, 6184.

[3] L. Yu, B. Yang, Q. Liu, J. Liu, X. Wang, D. Song, J. Wang, and X. Jing, *J. Electroanal. Chem.*, 2015, **739**, 156.

[4] S. Ratha, and C. S. Rout, *ACS Appl. Mater. Interfaces*, 2013, 5, 11427.

[5] Y. M. Dai, C. C. Wang, C. X. Zhang, H. H. Huang, S. H. Huang, P. Zuo, R. D. Xia, Y. X. Xia and X. K. Meng, *J. Alloys Compd.*, 2019, **805**, 631.

[6] X. M. Geng, Y. L. Zhang, Y. Han, J. X. Li, L. Yang, M. Benamara, L. Chen, and H. L. Zhu, *Nano Lett.* 2017, 17, 1825.

[7] A. Ramadoss, T. Kim, G. Kim and S. Kim, *New J. Chem.*, 2014, 38, 2379.

[8] L. Ma, L. M. Xu, X. P. Zhou, X. Y. Xu, and L. L. Zhang, *RSC Adv.*, 2015, **5**, 105862.

[9] P. Asen, M. Haghighi, S. Shahrokhian, and Nima Taghavinia, *J. Alloys Compd.*, 2019, **782**, 38.

[10] T. Zhang, L. B. Kong, M. C. Liu, Y. H. Dai, K. Yan, B. Hu, Y. C. Luo, and L. Kang, *Mater. Design*, 2016, **112**, 88.

[11] S. A. Ansari, and M. H. Cho, *Sustain. Energy Fuels*, 2017, **1**, 510.

[12] L. Wang, Y. Ma, M. Yang, and Y. X. Qi, *RSC Adv.*, 2015, **5**, 89069.

[13] H. Chauhan, M. K. Singh, S. A. Hashmib and S. Deka, *RCS Adv.*, 2015, **5**, 17228.

[14] Y. Li, H. Q. Xie and J. P. Tu, *Mater. Lett.*, 2009, **63**, 1785.

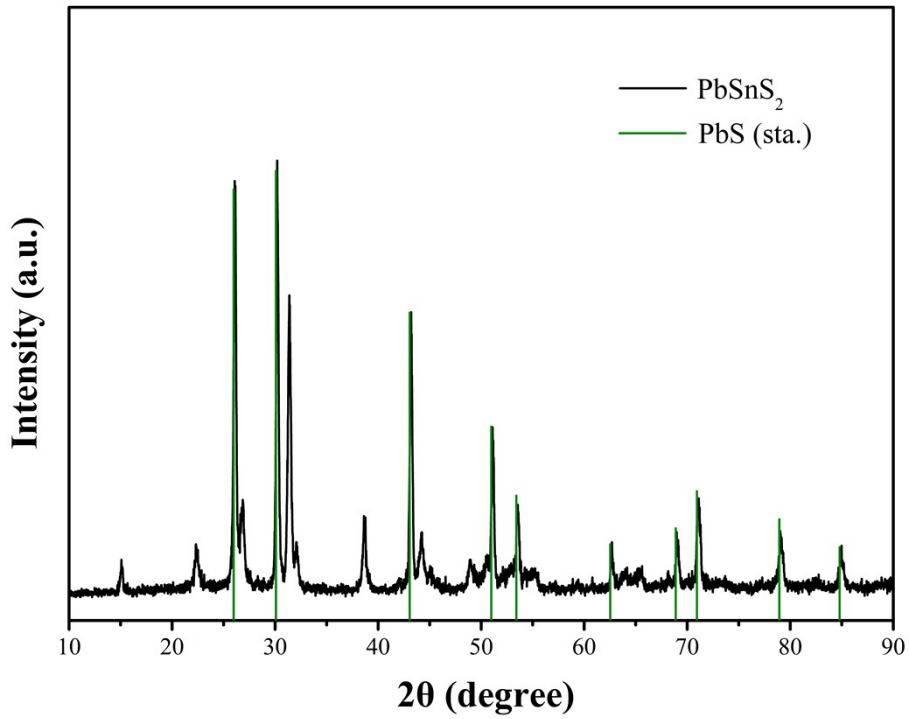

Fig. S1 XRD patterns of $PbSnS_2$ samples prepared at 180 °C, 6h. (The green lines represent the standard pattern of PbS)

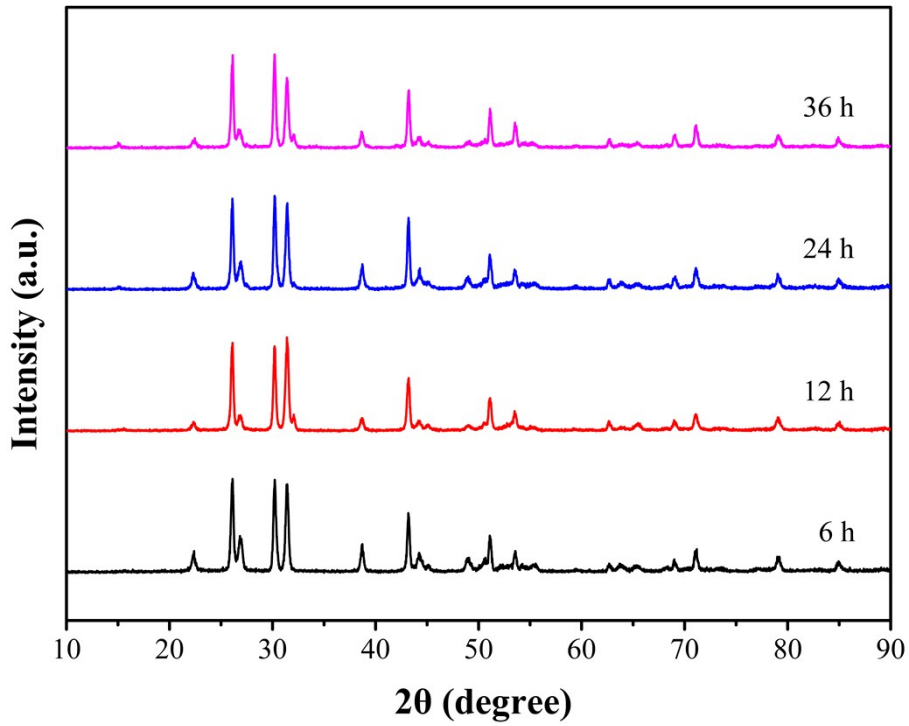

Fig. S2 XRD patterns of $PbSnS_2$ samples prepared at 160 °C after different reaction time.

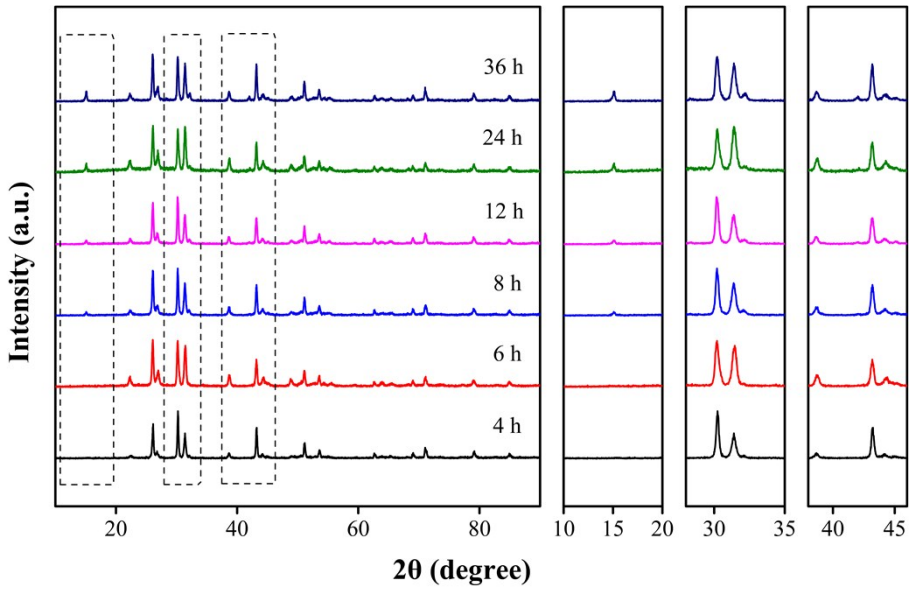

Fig. S3 XRD patterns of $PbSnS_2$ samples prepared at 180 °C after different reaction time.

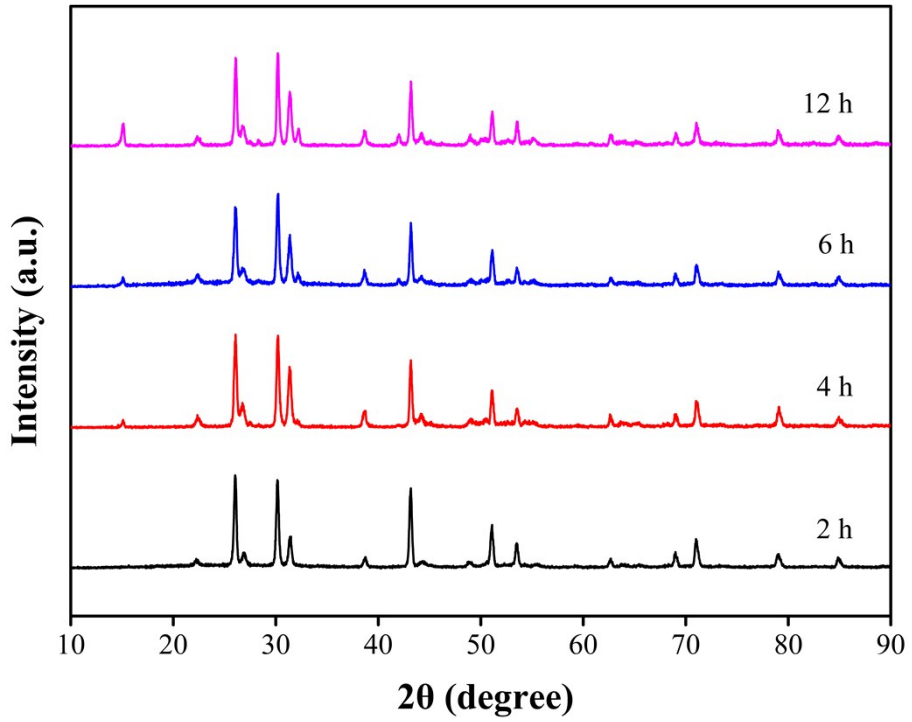

Fig. S4 XRD patterns of $PbSnS_2$ samples prepared at 200 °C after different reaction time.

Tab. S2 Measuring the values of 2-Theta of XRD for samples versus SnS (degree)

Time (hour)	Temperature (°C)				Standard SnS (intensity (%))
	160	180	200	220	
2			31.47	31.38	
4		31.40	31.34	31.38	
6	31.42	31.46	31.38	31.44	
8		31.38			31.53
12	31.40	31.38	31.36	31.42	(100)
18		31.46			
24	31.44	31.40			
36	31.40	31.40			

Tab. S3 Measuring the values of 2-Theta of XRD for samples versus PbS (degree)

Time (hour)	Temperature (°C)				Standard PbS (intensity (%))
	160	180	200	220	
2			51.10 69.03 71.00	51.10 69.03 71.02	
4		51.16 69.06 71.12	51.08 69.06 71.12	51.12 69.04 71.02	
6	51.08 69.00 71.08	51.10 69.03 71.12	51.12 69.02 71.12	51.16 69.06 71.16	
8		51.10 69.12 71.12			50.98 68.88 70.97
12	51.12 68.95 71.04	51.11 69.03 71.06	51.12 69.05 71.04	51.16 69.03 71.16	(100) (10) (17)
18		51.08 69.05 71.12			
24	51.06 69.03 71.08	51.10 68.98 71.12			
36	51.10 69.02 71.04	51.08 69.03 71.04			

The diffraction peak at 31.53° was corresponding to (111) plane of standard SnS sample and experimental results of this peak were shown in Tab. 2. According to Bragg's law, the smaller value of 2-Theta means lager interplanar spacing of (111) plane, proving the expansion of cells. This is rational because the larger radius of Pb atoms. Conversely, as shown in Tab. 3, the cell of PbS was contracting.[1] In terms of $PbSnS_2$, the diffraction peak measured in Tab. 2 also corresponded to the (111) plane of $PbSnS_2$, and the *c* axis of PbS was about half length of $PbSnS_2$ have mentioned previously.[2] These results indicated the cell volume change in PbS-SnS quasibinary system.

In this work, the cell dimensions were orthorhombic, a = 4.284 Å, b = 4.040 Å and c = 11.524 Å for $PbSnS_2$, orthorhombic, a = 4.268 Å, b = 4.051Å and c = 11.235 Å for SnS, and cubic, a = 5.854 Å for PbS. Obciously, SnS and PbS we obtained were impure, considered as $Pb_{2-x}Sn_xS_2$ ($1<x<2$) and $Pb_{2-x}Sn_xS_2$ ($0<x<1$) respectively. The shrinkage of calculated PbS and the expansion of calculated SnS were rational. After calculating, the volume of the unite cell increased by 3.3 % from the SnS to $PbSnS_2$.

[1] R. L. Orimia, H. K. Fadafan, and A. Asadpour, *Eur. Phys. J. Appl. Phys.*, 2014, **67**, 2040.

[2] K. Norton, J. Kunstmann, L. Ping, A. Rakowski, C. Wang, A. J. Marsden, G. Murtaza, N. Zeng, S. G. McAdams, M. A. Bissett, S. J. Haigh, B. Derby, G. Seifert, J. Chun-Ren Ke and D. *J. Lewis, Chem. Sci.*, 2019, **10**, 2843.

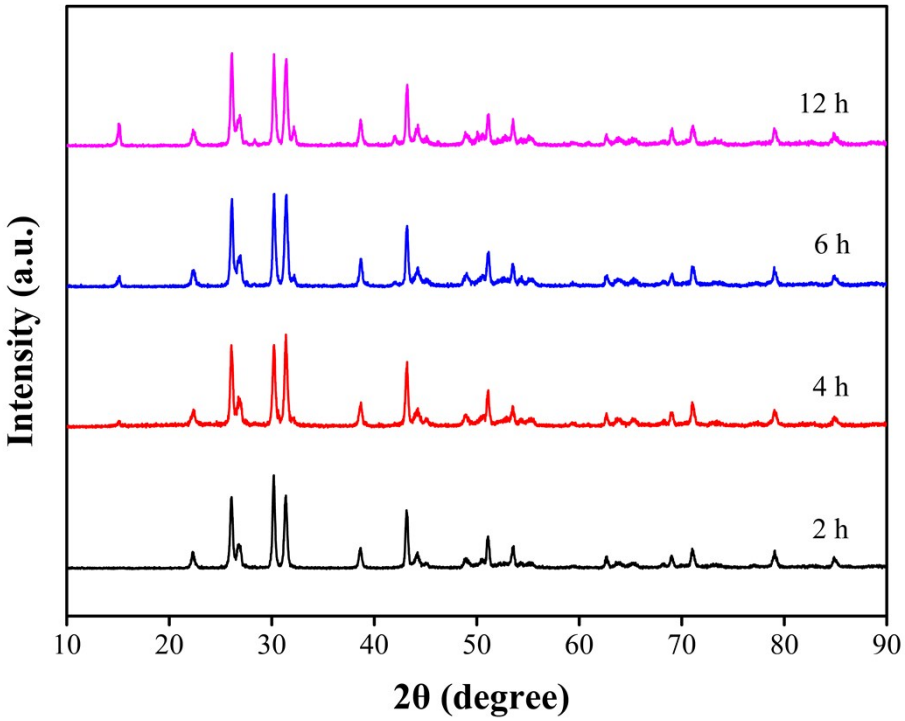

Fig. S5 XRD patterns of $PbSnS_2$ samples prepared at 220 °C after different reaction time.

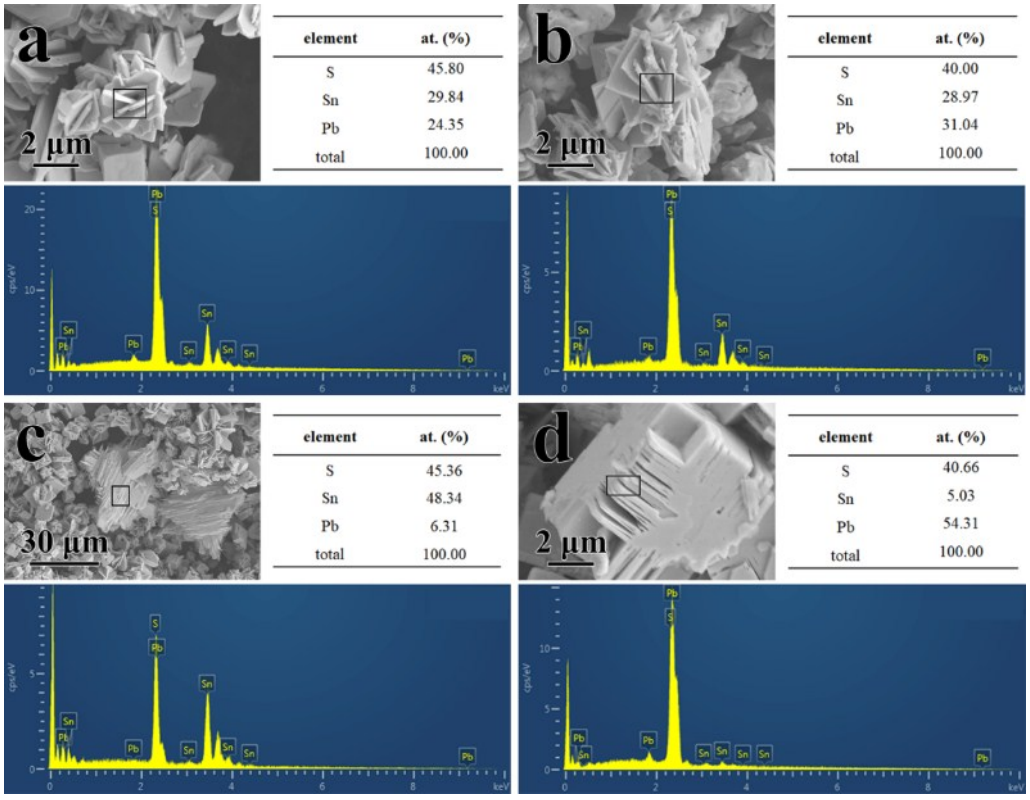

Fig. S6 SEM images, corresponding EDS spectra and the atomic ratio of each element of $Pb_{2-x}Sn_xS_2$, (a-b) x = 1, (c) 1<x<2, (d) 0<x<1.

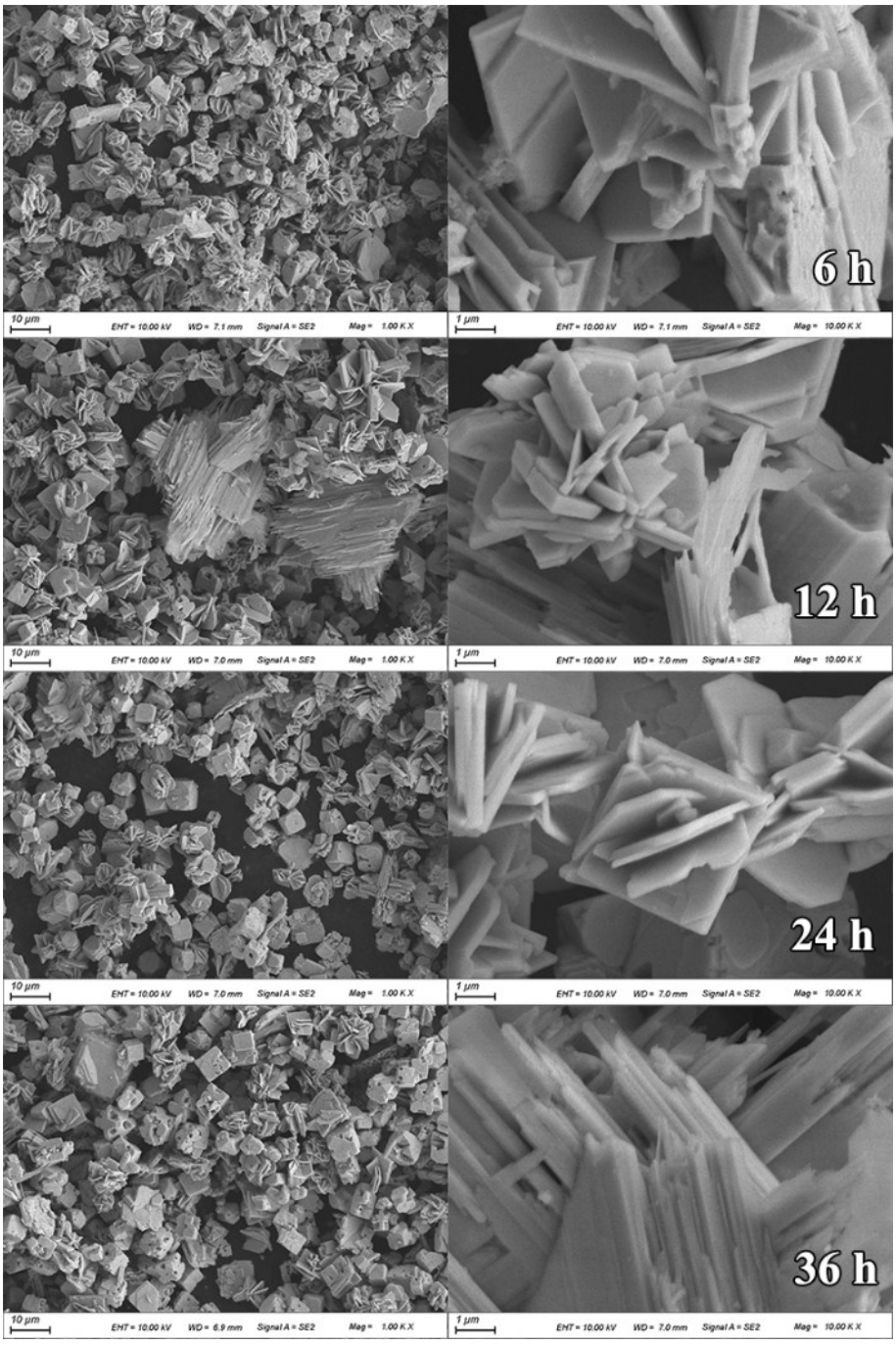

Fig. S7 SEM images of $PbSnS_2$ samples prepared at 160 °C after different reaction time.

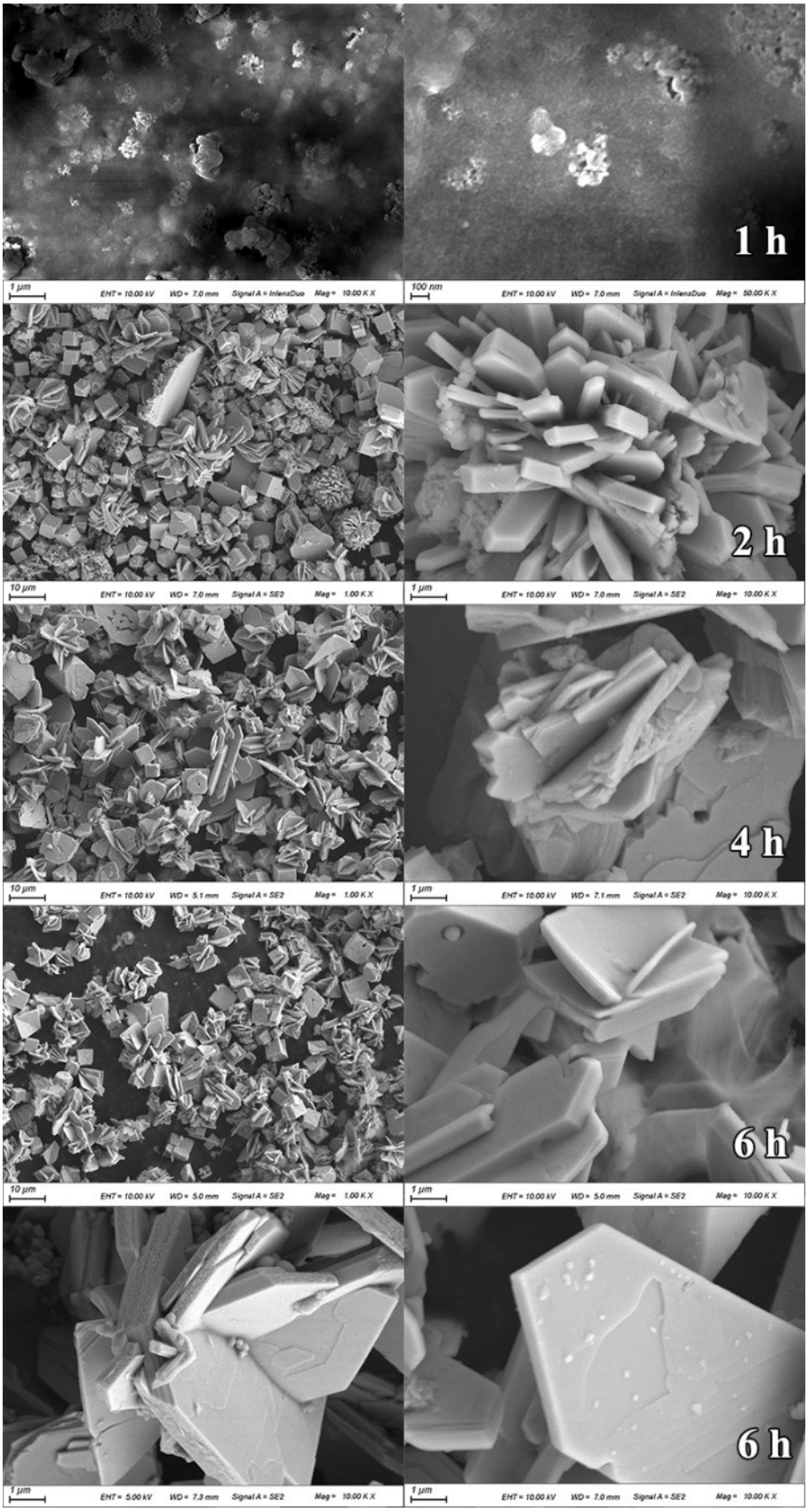
1 h
2 h
4 h
6 h
6 h

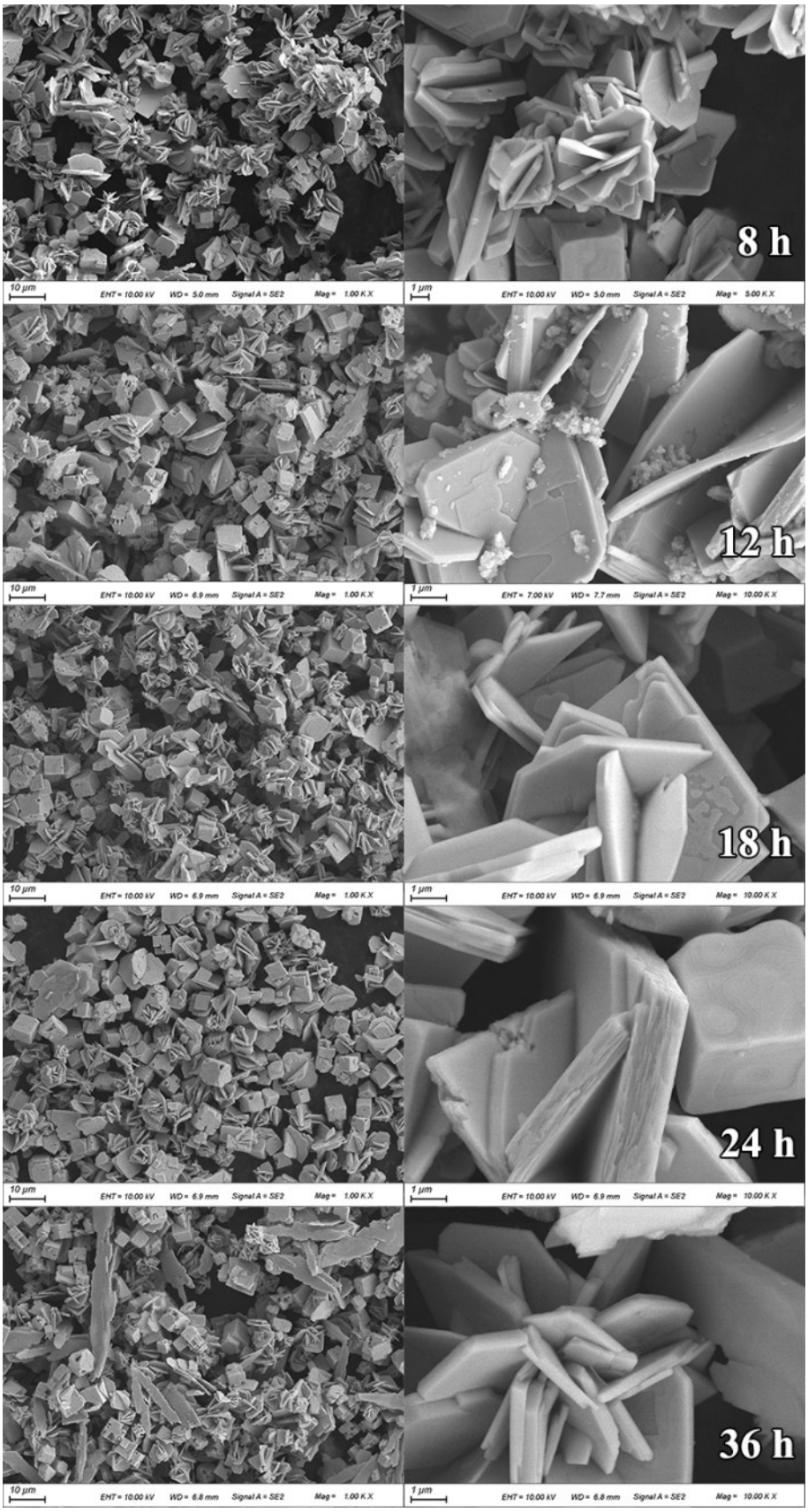

Fig. S8 SEM images of $PbSnS_2$ samples prepared at 180 °C after different reaction time.

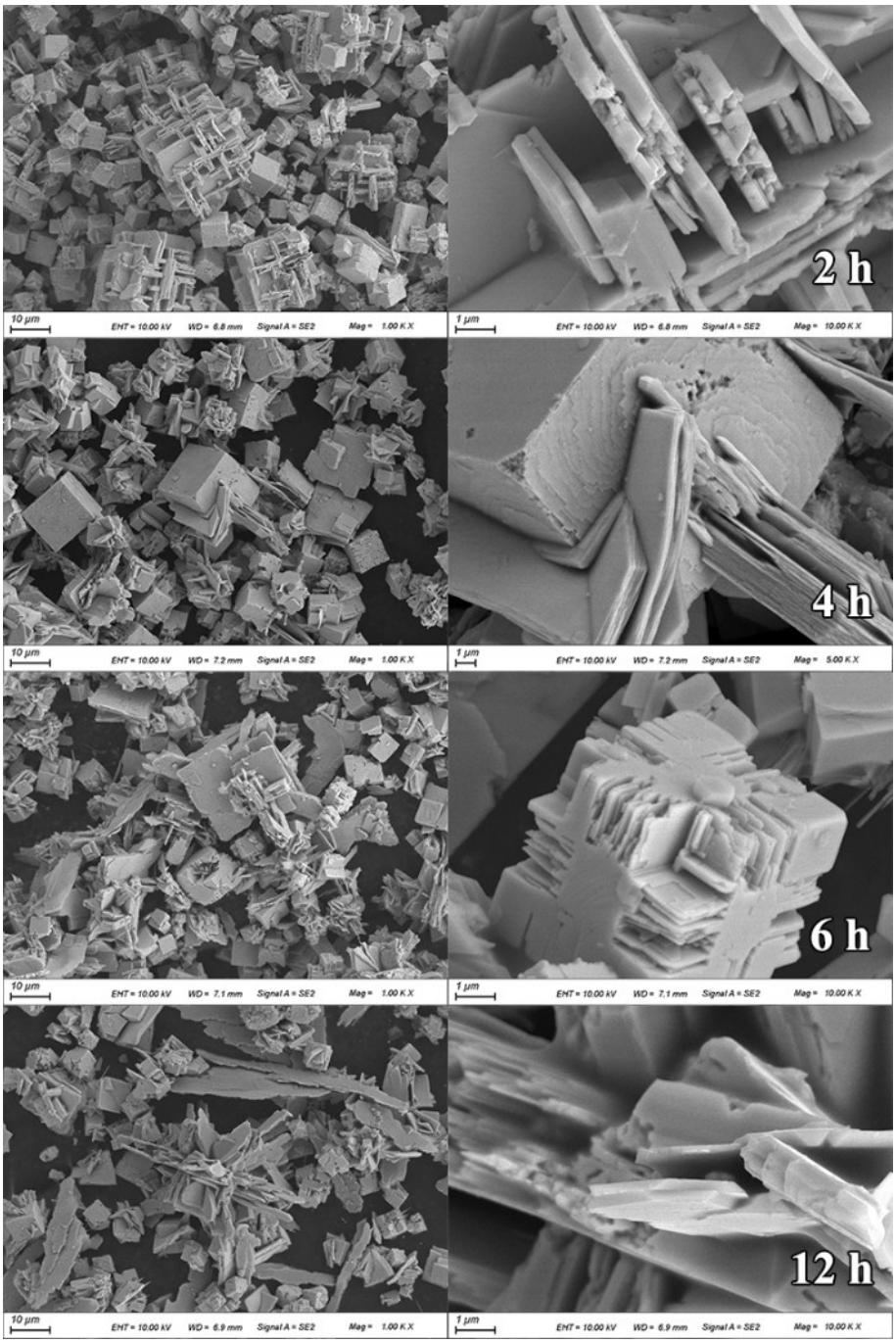

Fig. S9 SEM images of $PbSnS_2$ samples prepared at 200 °C after different reaction time.

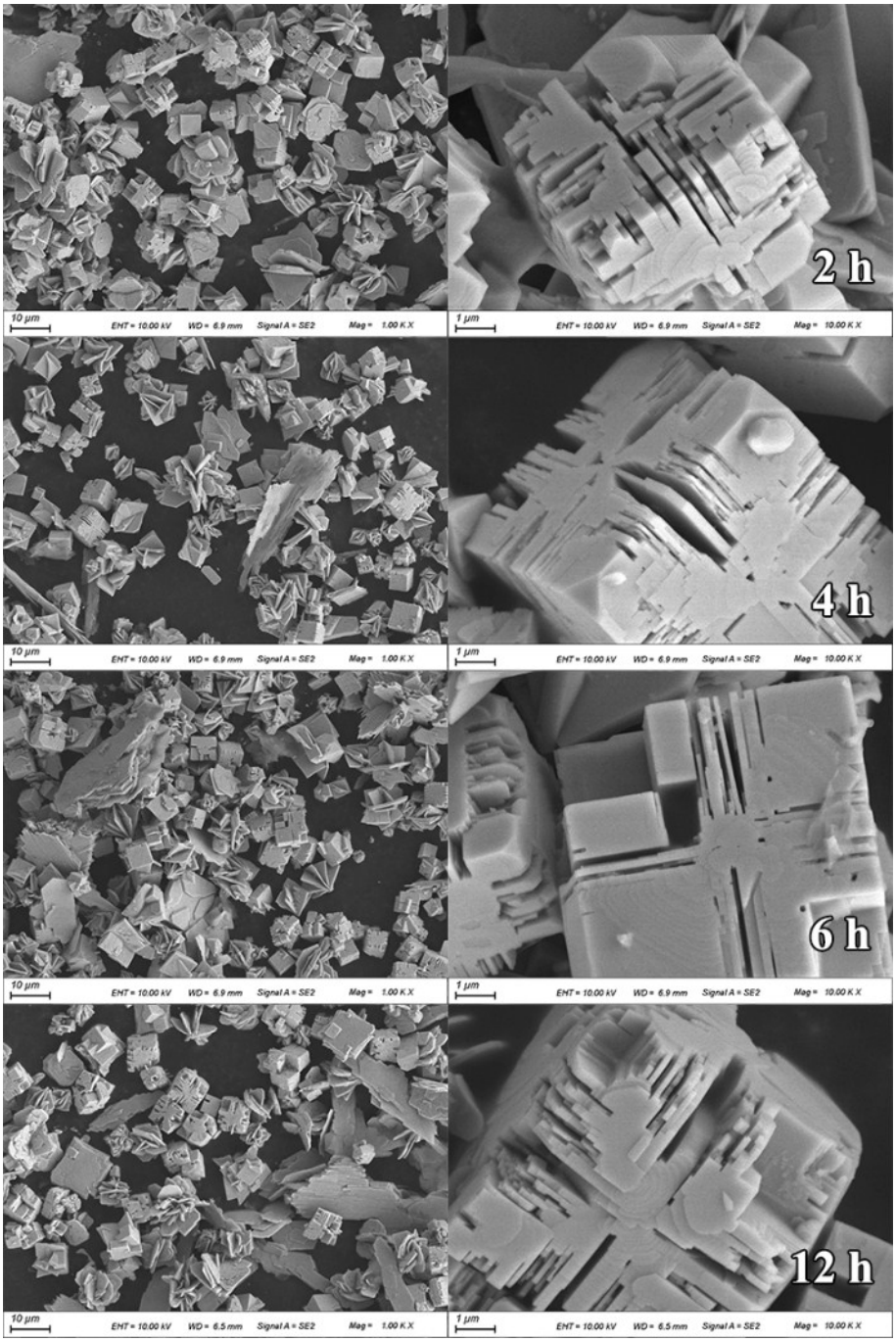

Fig. S10 SEM images of $PbSnS_2$ samples prepared at 220 °C after different reaction time.

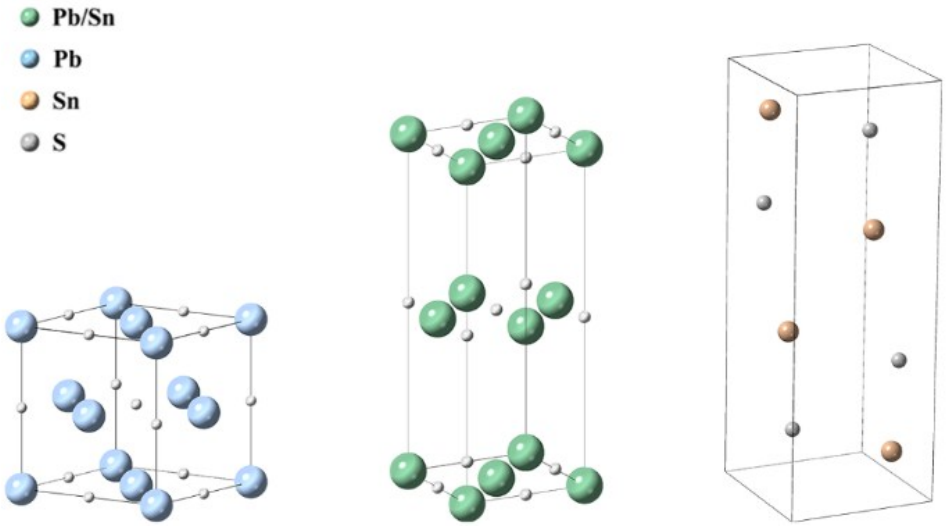

Fig. S11 Crystal structures of PbS, $PbSnS_2$ and SnS.

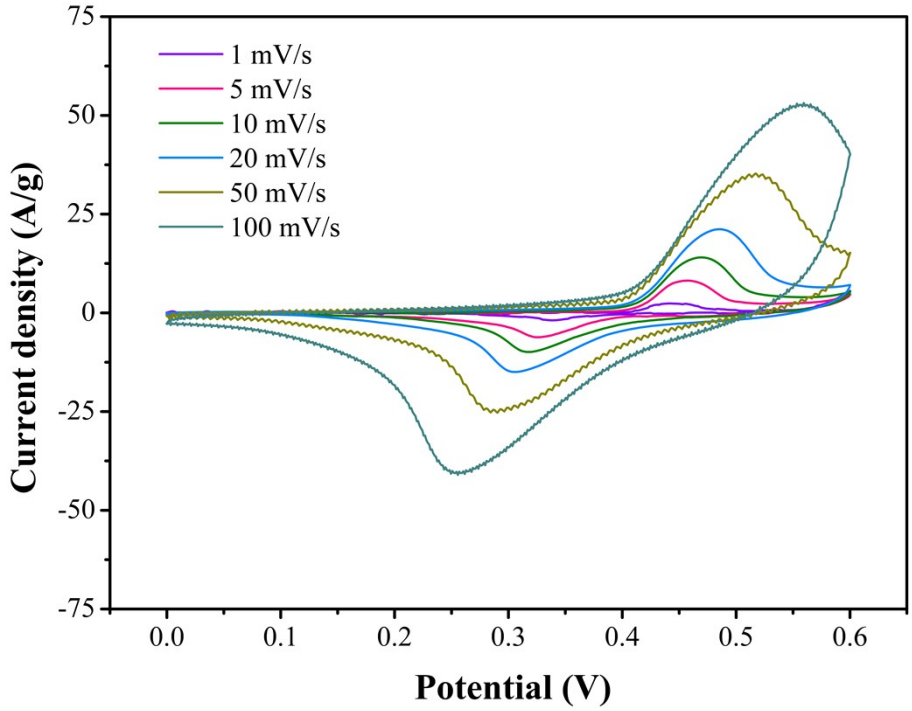

Fig. S12 CV curves of the pure SnS at different scan rates.

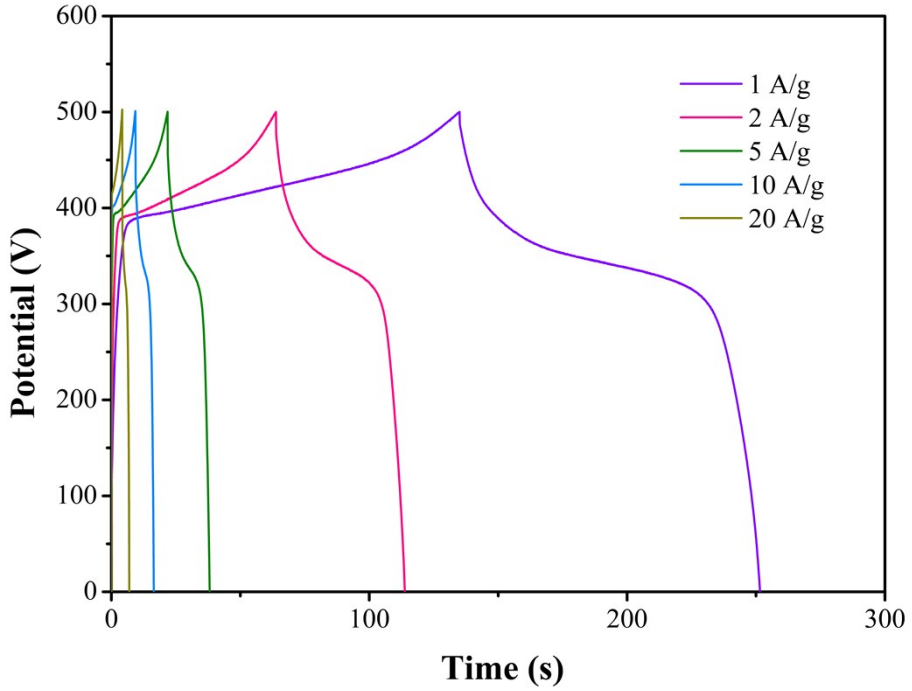

Fig. S13 GCD curves of the pure SnS at different current densities.

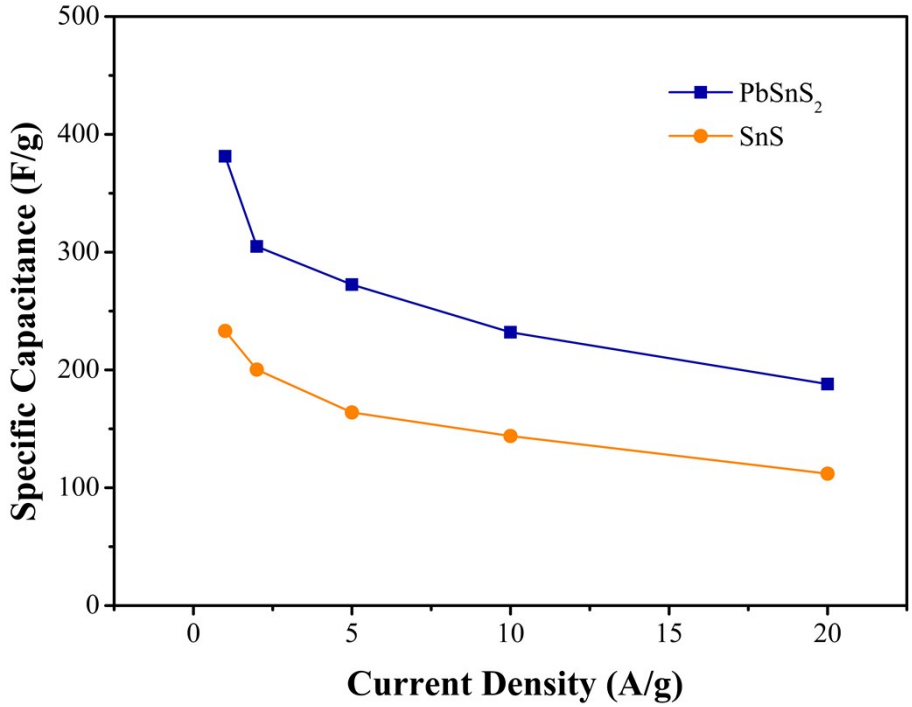

Fig. S14 Calculated the values of specific capacitance of $PbSnS_2$ and SnS samples at different current density.

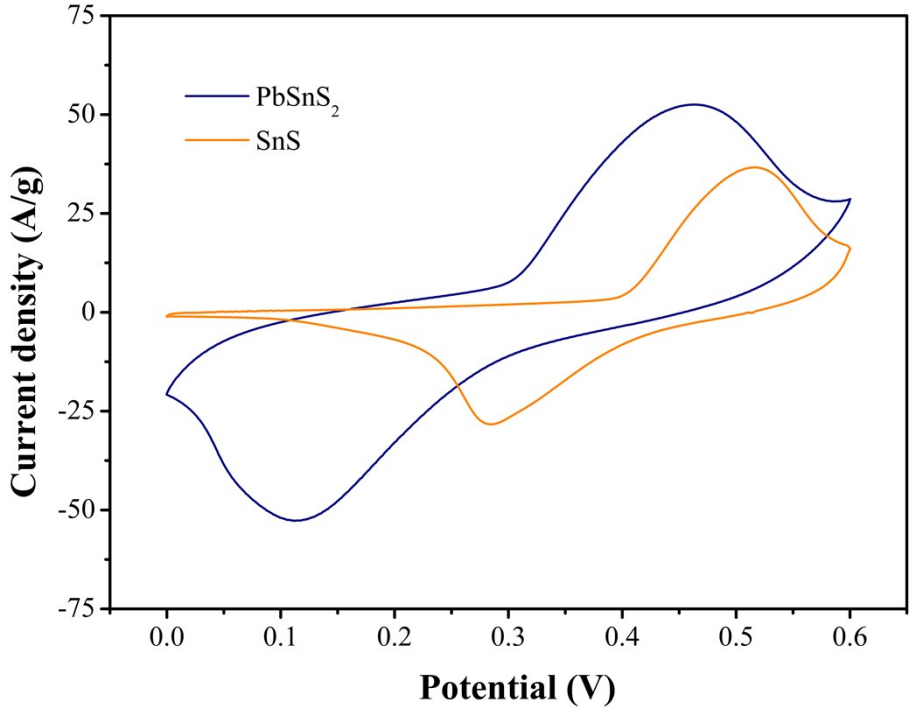

Fig. S15 CV curves of $PbSnS_2$ and SnS samples at 50 $mV \cdot s^{-1}$.

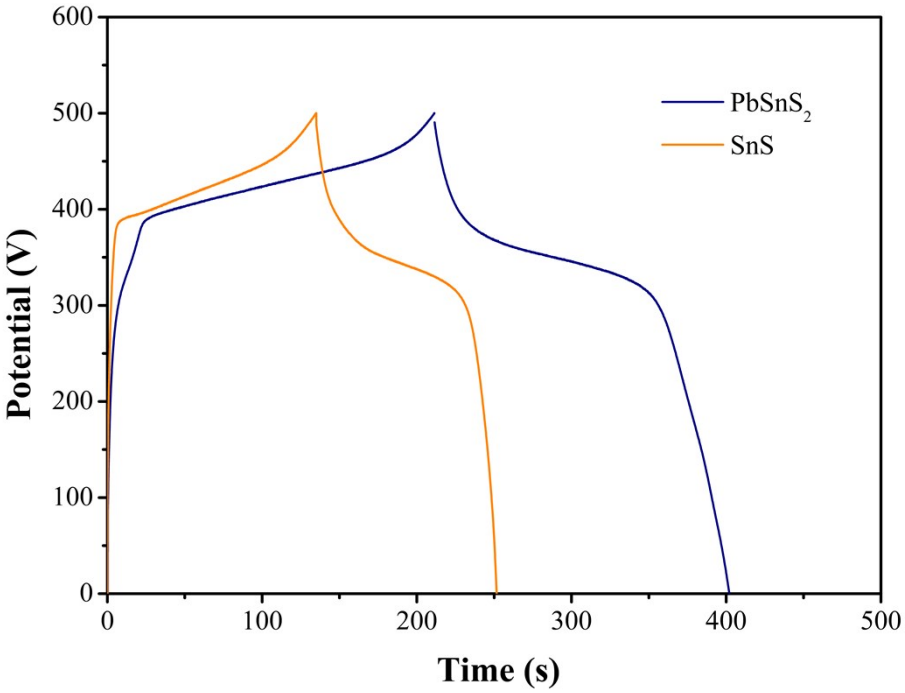

Fig. S16 GCD curves of $PbSnS_2$ and SnS samples at 5 $A \cdot g^{-1}$.

Fig. S17 The digital band illuminated with the $PbSnS_2$ electrode.